RESEARCH ARTICLE

Tangential Contact Stiffness Model of Solid-Liquid Interface Under Mixed Lubrication

LIXIA PENG [1,2]**, ZHAOYANG BAN**[3]**, ZHIQIANG GAO**[1]**, WEIPING FU** [1,2]**,
FENG GAO**[1]**, AND WEN WANG**[1]

[1] School of Mechanical and Precision Instrument Engineering, Xi'an University of Technology, Xi'an 710048, China
[2] School of Engineering, Xi'an International University, Xi'an 710061, China
[3] Xi'an Lingkong Electronic Technology Company Ltd., Xi'an 710000, China

Corresponding author: Lixia Peng (weipingf@xaut.edu.cn)

ABSTRACT In order to analyze and predict the performance of mechanical structure and system, the tangential contact of solid-liquid interface under normal and tangential loads is studied, and the tangential stiffness model of rough surfaces is established by analyzing various contact states of the asperity under normal elastic-plastic deformation and tangential stick-slip. Based on the contact model of closed oil pits based on the influence of rough surfaces, on the basis of fully considering the influence of gradual application of load on the number of closed oil pit, and then changing the load distribution of solid-liquid interface, a liquid tangential stiffness model is established. The tangential stiffness of solid-liquid interface is obtained by two parts in parallel. Through simulation and experimental analysis, the effects of normal load, deformation and lubricant viscosity on the tangential stiffness of solid-liquid interface are revealed, and the tangential stiffness with or without lubricating medium is compared and analyzed. The results show that the tangential stiffness of solid-liquid interface and solid-solid interface increases nonlinearly with the increase of normal load and deformation. Due to the contribution of liquid stiffness, the tangential stiffness of solid-liquid interface is always slightly higher than that of solid-solid interface. The greater the viscosity of the lubricating medium, the greater the tangential stiffness of the solid-liquid interface. At low load, liquid contact is dominant, and the tangential stiffness of solid-liquid interface is low. Under moderate and heavy loads, the solid contact is dominant, and the tangential stiffness of the solid-liquid interface increases rapidly. Therefore, the tangential contact stiffness of the solid-liquid interface in mixed lubrication can be effectively improved by increasing the normal load and increasing the viscosity of the lubricating medium.

INDEX TERMS Mixed lubrication, tangential contact stiffness, asperity, closed oil pit.

I. INTRODUCTION

There are a large number of mixed lubrication bonding surfaces in the core basic parts of mechanical transmission represented by gears, bearings and guideways [1], and their contact stiffness is one of the most important parameters used to describe the characteristics of the bonding surface.

The associate editor coordinating the review of this manuscript and approving it for publication was Hassen Ouakad.

The change of contact stiffness directly affects the static and dynamic characteristics of the joint and the mechanical equipment system, including contact pressure distribution, vibration and noise response characteristics, fatigue and wear characteristics and working stability [2], [3], [4], [5]. Therefore, the accurate calculation of tangential contact stiffness of solid-liquid interface under mixed lubrication is very important for the performance analysis and prediction of mechanical structure and system.

At present, the research on the tangential stiffness characteristics of rough contact interface has received extensive attention, and the statistical model and fractal model based on rough surfaces have been gradually formed [6], [7], [8], [9], [10], [11]. However, these models are solid-solid contact without lubricating media, and the effect of lubricating film on stiffness is not taken into account. In fact, the contact stiffness of the mixed lubrication interface is obviously affected by the surface morphology and lubrication performance [12]. Cheng et al. [13] divided the contact area into oil film contact area and rough contact area by determining the average oil film thickness and rough contact ratio, calculated the corresponding stiffness respectively, and synthesized the results of the two parts according to the rough contact ratio to obtain the normal stiffness of the mixed lubrication joint. Wang. et al. [14] proposed a method for calculating the time-varying contact normal stiffness of spiral bevel gears under transient mixed lubrication. The results show that there is a significant difference between transient mixed contact stiffness and solid-solid contact, indicating the importance of lubrication and rough contact. Dwyer-Joyce et al. [15] proposed a method based on ultrasonic reflection to measure the normal contact stiffness of lubricated steel balls from static, mixed to full-film states, and established a mixed lubrication process model including load distribution, rough contact and elastohydrodynamic film thickness. The model is used to predict liquid and rough stiffness components. Subsequently, Xiao et al. [16] further proposed the normal stiffness calculation model of hybrid elastohydrodynamic lubrication line contact, and concluded that the stiffness of lubricating film is much higher than that of solid contact, and dominates the total stiffness. Cheng et al. [17] improved Xiao's stiffness calculation model and obtained the numerical solution based on the hybrid elastohydrodynamic lubrication model, which better reflects the influence of rough surfaces and lubrication on gear meshing stiffness.

The studies above show that lubrication has a significant effect on the contact characteristics of the joint from the point of view of load distribution and the proportion of oil film stiffness, but they are all aimed at the normal direction, and there is little research on tangential contact stiffness under mixed lubrication. Because the friction performance of lubricating film is very different from that of solid contact, and varies with the change of working conditions, the tangential contact characteristics and normal direction of solid-liquid interface under mixed lubrication are fundamentally different and more complex.

According to the assumption that the surface shear stress of layered elements is equal, Changjiang Zhou et al. [18], [19] proposed the tangential stiffness model of oil film of spur gear under mixed lubrication, and further obtained the combined stiffness of solid-liquid interface. The effects of three basic parameters of gear transmission (contact force, speed and number of teeth) on the combined stiffness of line contact elastohydrodynamic lubrication are discussed

in detail. However, they study the working conditions of non-Newtonian elastohydrodynamic line contact, and the key problems of tangential contact such as the mechanism of load distribution between solid contact and liquid contact and the elastic-plastic deformation of solid contact remain to be solved.

In this article, under the combined action of normal force and tangential force, the solid-liquid interface under the mixed lubrication of surface contact based on Newtonian fluid viscosity theorem is taken as the research object. On the basis of fully considering the elastic/elastoplastic/plastic deformation of contact asperity and the influence of the change of the number of liquid closed oil pits on the mechanism of load distribution, the tangential stiffness of solid contact and liquid contact are established respectively. Then the comprehensive stiffness model is obtained. The established model is simulated and tested, the influencing factors and laws are clarified and revealed, the correctness of the theoretical model is verified, and compared with the solid contact characteristics, and the qualitative comparison conclusions are given. The purpose of this article is to provide a reference for improving the performance of the whole machine in the process of mechanical equipment design and manufacturing with lubricating medium.

II. SOLID-LIQUID PARALLEL CONTACT MODEL OF MIXED LUBRICATION INTERFACE

Based on the assumption of GW [20] model, the contact between two rough surfaces with lubricating medium is equivalent to the contact between a rough surface with lubricating medium and a rigid smooth plane, and the microscopic contact is equivalent as shown in Figure 1.
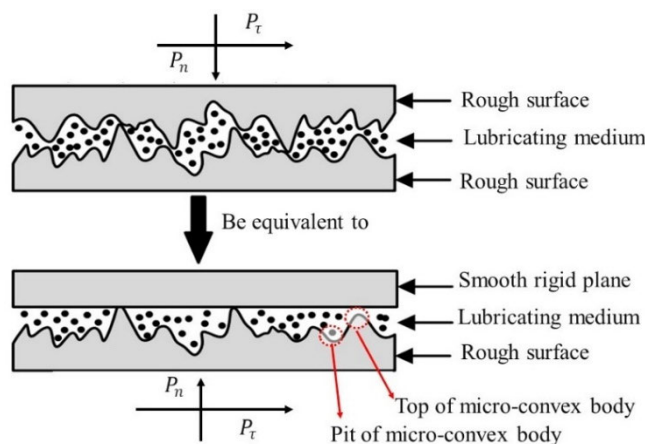
FIGURE 1. Equivalent diagram of contact of mixed lubrication interface.

When the rigid smooth plane and the rough plane are in contact with the normal load, according to the Mechanical-Rheological Model of the contact interface in the mixed state [21], the top of the asperity on the rough surface first bears the load to form a solid contact area, while the asperity pits on the

rough surface have a liquid contact area formed by lubricant, and the load is borne by both the asperity on the rough surface and the lubricant in the pit. Therefore, the tangential contact stiffness K_{sum} of solid-liquid interface is

$$K_{sum} = K_{\tau s} + K_{\tau l} \tag{1}$$

where $K_{\tau s}$ is the tangential stiffness of the solid contact part, while $K_{\tau l}$ is the tangential stiffness of the liquid contact part.

III. TANGENTIAL STIFFNESS OF SOLID CONTACT PART
A. NORMAL LOAD AND CONTACT AREA OF SOLID CONTACT PART

According to the finite element analysis of KKE Model [22], when two rough surfaces are in contact, the asperity will undergo elastic, elastic-plastic and plastic deformation under normal load. When $\delta < \delta_e$, the asperity is in the stage of elastic deformation; when $\delta_e < \delta < 110\delta_e$, the asperity is in the stage of elastic-plastic deformation; and when $110\delta_e < \delta$, the asperity is in the stage of complete plastic deformation. δ is the normal deformation of the asperity, and δ_e is the critical deformation of the asperity from the elastic stage to the elastic-plastic stage [23], which can be represented as

$$\delta_e = (\frac{3\pi kH}{4E})^2 R \tag{2}$$

where k is the critical yield stress coefficient, $k = 1.295e^{0.736\nu}$, H and ν are minimum values of hardness and Poisson's ratio of two surface materials, E is the equivalent elastic modulus of two rough surfaces, and R is the equivalent radius of curvature of the asperity.

When the height z of the asperity is in the range (d, ∞), the solid contact zone is formed, and the rest is the liquid contact zone, then the number of contact the asperity N is

$$N = A_n \rho \int_d^\infty \phi(z)dz \tag{3}$$

The total actual contact area and normal load of two rough surfaces can be represented as [24], [25], [26], [27]

$$A_s = \pi R \rho A_n \left\{ \begin{array}{l} \int_d^{d+\delta_e} \delta\phi(z)dz \\ + \int_{d+\delta_e}^{d+110\delta_e} \delta_e \left[1.19(\frac{\delta}{\delta_e} - 1)^{1.1} + 1\right]\phi(z)dz \\ + \int_{d+110\delta_e}^{+\infty} 2\delta\phi(z)dz \end{array} \right\} \tag{4}$$

$$P_{ns} = \frac{4}{3}ER^{\frac{1}{2}}\rho A_n \int_d^{d+\delta_e} \delta^{\frac{3}{2}}\phi(z)dz + \frac{4}{3}ER^{\frac{1}{2}}\delta_e^{\frac{3}{2}} \int_{d+\delta_e}^{d+110\delta_e}$$
$$\times \left[1.32(\frac{\delta}{\delta_e} - 1)^{1.27} + 1\right]\phi(z)dz$$
$$+ 2\pi RH \int_{d+110\delta_e}^{+\infty} \delta\phi(z)dz \tag{5}$$

where A_n is the nominal contact area of the contact surface, ρ is the area density of the asperity, d is the distance between two rough surfaces, z is the height of the asperity, and $\phi(z)$ is

the probability density function of the asperity distribution; therefore the assumption obeys the Gaussian distribution.

B. TANFENTIAL LOAD AND STIFFNESS OF SOLID CONTACT PART

From the Cattaneo-Mindlin [28], [29] Model, it is known that the asperity forms a circular contact area with a radius of $r(r = (\frac{3RP_n}{4E})^{\frac{1}{3}})$ under the action of normal load P_n. Suppose the friction coefficient of the contact area is μ, and the tangential displacement ξ is produced under the application of tangential static load P_τ. Due to the non-uniform distribution of contact pressure on the contact area, a viscous zone with radius $c(c = r(1 - \frac{P_\tau}{\mu P_n})^{\frac{1}{3}})$ and a micro-slip zone with radius $r - c$ will be formed. These two regions constitute the stable contact state of the asperity; that is, the stick-slip contact state of the asperity, as shown in Figure 2. When there is no tangential load, the viscous area is full of the contact surface of the asperity. Under the continuous application of the tangential force, the slip zone expands from the contact edge to the center of the circle to the whole contact surface, and the slip zone occupies the whole contact surface. Then the asperity appears macroscopic movement state. This article considers the static contact in the mixed lubrication state, that is, the stick-slip contact state of the asperity.
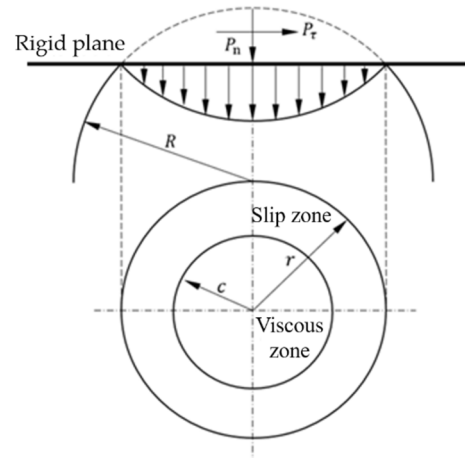
FIGURE 2. Stick-slip contact model of asperity.

According to theories of Mindlin [29] and Fojimoto [26], as well as [27], [28], [30], and [31], the asperity is in the stage of elastic, elastic-plastic and plastic deformations, and therefore the tangential loads $P_{\tau e}$, $P_{\tau ep}$, and $P_{\tau p}$ can be represented as

$$P_{\tau e} = \left\{ \begin{array}{ll} \mu P_{ne}\left[1 - (1 - \frac{\xi}{\xi_e})^{\frac{2}{3}}\right] & \xi \leq \xi_e \\ \mu P_{ne}, \xi > \xi_e, \end{array} \right. \tag{6}$$

$$P_{\tau ep} = \left\{ \begin{array}{ll} \mu P_1\left[1 - (1 - \frac{\xi}{\xi_{eep}})^{\frac{3}{2}}\right] + \frac{\mu P_2 \xi}{\xi_{pep}}, & \xi \leq \xi_{eep} \\ \mu P_{nep}, & \xi > \xi_{eep} \end{array} \right. \tag{7}$$

$$P_{\tau p} = \begin{cases} \dfrac{\mu P_{np}\xi}{\xi_p}, & \xi \leq \xi_p \\ \mu P_{np}, & \xi > \xi_p \end{cases} \qquad (8)$$

where G is the equivalent shear modulus of two rough surfaces and v is the equivalent Poisson's ratio. ξ_e, ξ_{eep} and ξ_p are the critical displacements of the asperity from the viscous state to the micro-slip state in the elastic, elastic-plastic and plastic deformation stages, respectively. Therefore, $\xi_e = \mu E(2 - v)\delta/4G$, $\xi_{eep} = \frac{3(2-v)\mu P_1}{16Gr}$, $\xi_p = \mu H(2R\delta)^{\frac{1}{2}}/2G$; $P_1 = 2\pi \int_{a_p}^{a} p(r)rdr$, $P_2 = \pi a_p^2 p_y$, $p(r) = \frac{3P_{nep}}{2\pi a^2}\left[1 - (\frac{a}{r})^2\right]^{\frac{1}{2}}$, $a_p^2 = r^2 - (\frac{\pi Rp_y}{2E})^2$, $r = (\frac{3RP_{nep}}{4E})^{\frac{1}{3}}$, p_y is yield stress of interface material, $\xi_{pep} = \frac{\mu}{2G}(\frac{H}{\pi})^{\frac{1}{2}}P_2^{\frac{1}{2}}$.

$$K_{\tau e} = \frac{\partial P_{\tau e}}{\partial \xi} = \frac{2\sqrt{R}\delta^{\frac{3}{2}}\mu\sqrt{1 - \frac{\xi}{\xi_e}}}{\xi_e} \qquad (9)$$

$$K_{\tau ep} = \frac{dP_{\tau ep}}{d\xi} = \frac{8Gr}{2 - v}\sqrt{1 - \frac{\xi}{\xi_{eep}}} + \frac{2}{3}G\sqrt{P_2}\sqrt{\frac{\pi}{H}} \qquad (10)$$

$$K_{\tau p} = \frac{dP_{\tau p}}{d\xi} = 2\sqrt{2}\pi G\sqrt{R\delta} \qquad (11)$$

In the micro-slip state, the tangential stiffness is zero. By extending the above single asperity stiffness model to the whole solid interface, it is obtained that the tangential total stiffness $K_{\tau s}$ of the solid contact part is

$$K_{\tau s} = N(K_{\tau e} + K_{\tau ep} + K_{\tau p}) \qquad (12)$$

IV. TANGENTIAL STIFFNESS OF LIQUID CONTACT PART

The pits in the liquid contact area will form two different forms: open oil pits and closed oil pits. The open oil pit is connected with the boundary of the contact interface, and with the increase of load, the lubricant in the open oil pit is extruded to form hydrodynamic pressure, which is a load balance process before the static state of the joint, which generally does not need to be considered. The closed oil pits are not connected with the boundary of the contact interface, and when squeezed, the lubricant is trapped in these pits, resulting in hydrostatic pressure to bear part of the normal load. With the increase of normal load, the asperity will gradually experience elastic deformation, elastic-plastic deformation and plastic deformation, and the solid contact area will gradually increase and begin to connect with each other, thus forming a new closed oil pit. Therefore, the appearance of closed oil pits at the contact interface is the main factor to change the load distribution mechanism on the solid-liquid interface.

A. TANGENTIAL SINGLE CLOSED OIL PIT MODEL

As shown in Figure 3, the closed oil pit contact model makes the following assumptions:

(1) The closed oil pit is a hemisphere with a radius of R_1.

(2) After loading, the average height of the surrounding asperity decreases, the closed oil pit becomes a semi-ellipsoid, and the contact area of the upper end face remains

unchanged; that is, the radius of curvature R_1 on the end face remains unchanged.

(3) After being extruded by the normal rigid plane, the volume of the closed oil pit becomes smaller, the distance in the normal direction becomes shorter, and the shorter distance is δ_l.

(4) Under general working conditions, most lubricants, especially mineral oils, belong to Newtonian fluid properties. That is to say, the lubricant in the closed oil pit is Newtonian fluid and compressible fluid, and the temperature change is not obvious after loading; that is, the viscosity-temperature relationship is not considered.
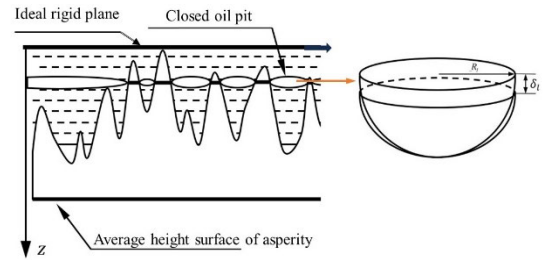
FIGURE 3. Closed oil pit contact model.

1) VISCOSITY-PRESSURE RELATIONSHIP

According to the Reference [32], we can use the Reoland viscosity-pressure relationship, and compared with the Barus viscosity-pressure relationship, the Reoland viscosity-pressure relationship is more related to the actual situation, that is:

$$\eta_p = \eta_0 \exp\left\{(\ln \eta_0 + 9.67)\left[-1 + (1 + \frac{P}{P_0})^z\right]\right\} \qquad (13)$$

where η_p is the viscosity at pressure P; η_0 is the viscosity at the standard atmospheric pressure $P_0 = 5.1 \times 10^{-9}$; for general mineral oil, the value of z can usually be up 0.68.

2) DENSITY-PRESSURE RELATIONSHIP

By considering the variation of lubricating oil density with pressure, Dowson and Higginson regressed the following experience formula of density-pressure [33].

$$\rho_p = \rho_0(1 + \frac{D_1 P_{nli}}{1 + D_2 P_{nli}}) \qquad (14)$$

where ρ_0 and ρ_p are the densities at P_0 and P_{nli}. D_1 and D_2 are the constants, 0.6 GPa^{-1}, 1.7 GPa^{-1} respectively. These two constants are basically applicable to all lubricants.

Before extruded, the closed oil pit is hemispheric and its volume is:

$$V_s = \frac{2}{3}\pi R_l^3 \qquad (15)$$

$$V_e = \frac{2}{3}\pi R_l^2(R_l - \delta_l) \qquad (16)$$

In the absence of leakage, the mass before and after extrusion by normal force can be obtained from the mass

conservation of lubricant, that is

$$\rho_0 V_s = \rho_p V_e \qquad (17)$$

By substituting Equations 14-16 into Equation 17, the relationship between the normal pressure and the deformation of the closed oil pit can be obtained.

$$P_{nli} = \frac{\delta_l}{1.7\delta_l - 0.6R_l} \qquad (18)$$

3) FRICTION FORCE OF CLOSED OIL PIT

When According to Newton's Law of Viscosity [32], the friction force $P_{\tau li}$ on the upper end of the closed oil pit is

$$P_{\tau li} = \tau A_{ti} \qquad (19)$$

where A_{ti} is the area of the upper end of the closed oil pit, whose value is πR_l^2; τ is the viscous shear stress of Newtonian fluid on the upper face of the closed oil pit, and the equation is

$$\tau = \eta_p \frac{du}{dz} \qquad (20)$$

where $\frac{du}{dz}$ is the gradient of the flow velocity of the lubricating film along the direction of the fluid thickness. In this article, the research object is in the state of stick-slip contact in tangential direction, and there is only micro-slip displacement ξ. If the time experienced is t, the velocity of lubricating film on the upper end face of the closed oil pit is $u = \xi/t$, the velocity at the lower end face is zero, and the thickness of lubricating film h_l is very thin, then the Equation (20) can be equivalent to

$$\tau = \eta_p \frac{u}{h_l} \qquad (21)$$

By substituting the Equations (21), (13) and (18) into Equation (19), the friction force $P_{\tau li}$ on the upper end of the closed oil pit can be obtained as follows:

$$P_{\tau li} = \pi \eta_0 R_l^2 \exp\left\{ \begin{array}{c} (\ln \eta_0 + 9.67) \\ \times \left[-1 + (1 + \frac{\delta_l}{P_0(0.6R - 2.3\delta_l)})^z \right] \end{array} \right\} \frac{u}{h_l} \qquad (22)$$

The tangential stiffness $K_{\tau li}$ of the closed oil pit can be derived from the tangential friction $P_{\tau li}$ versus its tangential displacement ξ, which can be represented as

$$K_{\tau li} = \frac{dP_{\tau li}}{d\xi}$$
$$= \pi \eta_0 R_l^2 \exp\left\{ \begin{array}{c} (\ln \eta_0 + 9.67) \\ \times \left[-1 + (1 + \frac{\delta_l}{P_0(0.6R - 2.3\delta_l)})^z \right] \end{array} \right\} / h_l t \qquad (23)$$

According to Reference [12], under the static contact state of mixed lubrication, the thickness of oil film can correspond to the equivalent deformation of rough surfaces.

B. MODEL OF INTEGRAL CLOSED OIL PIT ON ROUGU SURFACE

The area of liquid contact area on rough surfaces is the sum of all closed oil pits, which can be represented as

$$A_l = A_n - A_s \qquad (24)$$

In the process of gradually applying the normal load, the distance between the two rough surfaces gradually reduces, and the relatively shallow open oil pit at the bottom will be closed by extrusion pressure, so the number of closed oil pits will gradually accumulate with the application of the normal load.

Suppose the normal deformation be ε when all the normal load P_n is applied, that is, the normal deformation $0 \leq \delta \leq \varepsilon$. That is to say, the average height plane of the applied asperity is d_f; that is, $d = d_f + \varepsilon$, where $\varepsilon = \lambda i$ (λ is the step size, i is the loading stage when the asperity is gradually subjected to normal load, and the $i = 1, 2, \ldots \ldots n$).

$$M = \frac{A_l(d_f + \varepsilon) - A_l(d_f)}{A_t} = \frac{A_l(d) - A_l(d_f)}{\pi R_l^2} \qquad (25)$$

By substituting the Equation (4) into Equation (25), M can be calculated.

The normal load of all closed oil pits is

$$P_{nl} = M P_{nli} = \frac{\left[A_l(d) - A_l(d_f) \right] \delta_l}{\pi R_l^2 (1.7\delta_l - 0.6R_l)} \qquad (26)$$

The tangential friction of the liquid contact part is the joint action of all closed oil pits, which is shown as follows:

$$P_{\tau l} = M P_{\tau li} = \eta_0 \left[A_l(d) - A_l(d_f) \right]$$
$$\times \exp\left\{ \begin{array}{c} (\ln \eta_0 + 9.67) \\ \times \left[-1 + (1 + \frac{\delta_l}{P_0(0.6R - 2.3\delta_l)})^z \right] \end{array} \right\} \frac{u}{h_l} \qquad (27)$$

The tangential stiffness of the liquid contact part is

$$K_{\tau l} = M K_{\tau li} = \eta_0 \left[A_l(d) - A_l(d_f) \right]$$
$$\times \exp\left\{ (\ln \eta_0 + 9.67) \right.$$
$$\left. \times \left[-1 + (1 + \frac{\delta_l}{P_0(0.6R - 2.3\delta_l)})^z \right] \right\} / (h_l t) \qquad (28)$$

The tangential contact stiffness K_{sum} of solid-liquid interface can be obtained by bringing Equations (12) and (28) into Equation (1).

V. SIMULATION ANALYSIS OF TANGENTIAL STIFFNESS OF SOLID-LIQUID INTERFACE

The mechanical property parameters of contact surface are $E_1 = E_2 = 2.07 \times 10^{11}$Pa, Poisson's ratio $v_1 = v_2 = 0.29$, yield strength of material $p_y = 18$ GPa, standard deviation of height distribution of rough surfaces $\sigma = 1.89 \times 10^{-6}$, radius of curvature $R = R_l = 6.89 \times 10^{-4}$, nominal contact area $A_n = 7.07 \times 10^{-4}$ m^2, rough surface topography parameter $\beta = 0.14$, asperity density $\rho = 100 \times 10^{11}$ m^{-2}, time taper

t = 0.2 s, normal deformation $\delta = \delta_l$, lubricating oil dynamic viscosity parameters $\eta_{p1} = 80$ mPa · s, $\eta_{p2} = 150$ mPa · s, and $\eta_{p3} = 210$ mPa · s. The parameters in the simulation diagram are dimensionless and expressed by ∗.

A. RELATIONSHIP BETWEEN CONTACT LOAD AND NORMAL DEFORMATION OF CLOSED OIL PIT

Figure 4 shows the relationship between the contact load and the normal deformation of closed oil pit when the plasticity index is $\psi_3 = 2.5$. It can be seen from the figure that the normal load of the closed oil pit increases with the increase of deformation. This is because the normal deformation increases, the contact area of the solid contact part increases, the bearing proportion of the asperity increases, and the area of the liquid contact part decreases, so the load-bearing specific gravity of the closed oil pit decreases. However, the total load is still increasing, so the load of the closed oil pit is still increasing, which is qualitatively consistent with the results of Reference [34]. In addition, when the normal deformation is the same, the higher the viscosity is, the greater the load of the closed oil pit is.
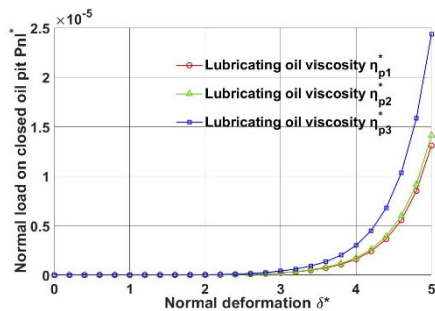
FIGURE 4. Relationship between normal load and normal deformation of closed oil pit.

B. RELATIONSHIP BETWEEN VISCOSITY AND NORMAL DEFORMATION OF CLOSED OIL PIT

Figure 5 shows the relationship between the viscosity of the closed oil pit lubricant and the normal deformation. It can be seen from the figure that the viscosity of the lubricant increases with the increase of normal deformation, which is due to the increase of normal deformation. From the conclusion of Figure 5, it can be seen that the normal load of the closed oil pit increases, so the viscosity increases.

C. RELATIONSHIP BETWEEN TANGENTIAL CONTACT STIFFNESS AND NORMAL DEFORMATION

Figure 6 shows the relationship between tangential contact stiffness and normal deformation under different plasticity index and lubricant viscosity. It can be seen from the diagram that the tangential contact stiffness of solid-solid interface and solid-liquid interface increases nonlinearly with the normal deformation, and the increase is accelerated after the normal deformation δ^* is 3.5. When the normal deformation is the same, the tangential contact stiffness of solid-liquid interface
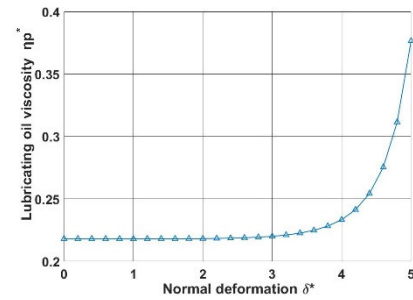
FIGURE 5. Relationship between lubricating oil viscosity and normal deformation of closed oil pit.

is larger than that of solid-solid interface, and the larger the plasticity index is, the greater the tangential stiffness of solid-solid interface is, and the greater the viscosity of lubricant is, the greater the tangential contact stiffness of solid-liquid interface is. This is because with the increase of normal deformation, the contact area of the solid contact part increases, and more asperity bodies will contact on the bonding surface, and the number of asperity bodies resisting deformation increases under the same tangential load. Therefore, the ability to resist deformation is enhanced; that is, the tangential contact stiffness of solid-solid interface and solid-liquid interface increases. For the solid-liquid interface, when the normal deformation is small; that is, under light load, the contact area of the solid contact part is smaller, and the liquid contact area is larger, at this time, the liquid contact is dominant, but the viscous friction force of the lubricant is still very small compared with the solid, so the overall tangential stiffness of the solid-liquid interface is slight. With the gradual application of normal load, the amount of normal deformation increases. Under medium and heavy load conditions, there are more and more asperity contact. At this time, the contact characteristics of solid-liquid interface are mainly dominated by solid contact, so when the normal deformation $\delta^* > 3.5$, the tangential contact stiffness of solid-liquid interface increases rapidly. The normal deformation continues to increase, and there are more and more contact asperity bodies, almost all of which are solid contact, so the stiffness variation curves of solid-solid interface and solid-liquid interface are gradually close to coincidence.

D. RELATIONSHIP BETWEEN TANGENTIAL CONTACT STIFFNESS AND NORMAL CONTACT LOAD

Figure 7 shows the relationship between tangential contact stiffness and normal contact load in the case of different plasticity index and lubricant viscosity. It can be seen from the figure that the tangential contact stiffness of the solid-solid interface increases nonlinearly with the normal contact load, which is consistent with the results of the [35] and [36], and the solid-liquid interface also shows the same trend. The tangential contact stiffness of solid-solid interface is always lower than that of solid-liquid interface. The higher the plasticity index and the higher the lubricant viscosity,
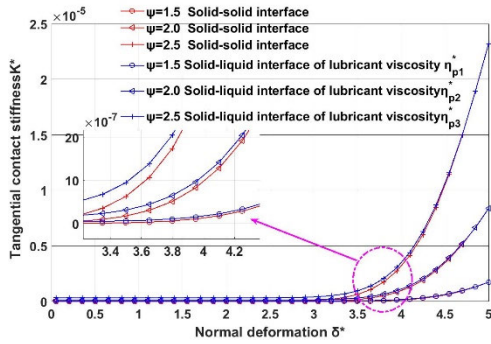
FIGURE 6. Relationship between tangential contact stiffness and normal deformation.

the greater the tangential contact stiffness of the solid-liquid interface. With the increase of normal contact load, the distance between bonding surfaces decreases gradually, the contact area of solid contact increases, the number of contact asperityity increases, and the ability to resist deformation increases, so whether it is solid-solid interface or solid-liquid interface, tangential contact stiffness will gradually increase. In addition, when the normal load is small, due to the contribution of the stiffness of the closed oil pit in the liquid contact part, the tangential stiffness of the solid-liquid interface is always larger than that of the solid-solid interface, and with the increase of the normal load, the solid contact gradually occupies the whole interface, so the tangential stiffness curve of the solid-liquid interface is gradually close to that of the solid-solid interface.
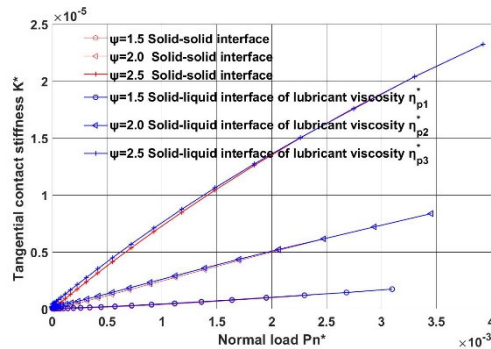
FIGURE 7. Relationship between tangential contact stiffness and normal load.

VI. EXPERIMENTAL VERIFICATION
In this article, based on the experimental platform built by Fu et al. [25], [37], the tangential contact characteristics of solid-liquid interface are experimentally analyzed. As shown in Figure 8, the tangential joint is composed of the left and right specimens in contact with the intermediate specimens.

By rotating the normal force screw, the normal load in the horizontal direction is given. Then the tangential force screw is rotated and the tangential load is applied step by step in the vertical direction. the tangential plane pressure and tangential

relative displacement signals are obtained according to the tangential static force sensor and eddy current displacement sensor. Then the normal load is applied step by step in the horizontal direction, and the previous tangential loading mode is repeated, and the normal surface pressure and tangential relative displacement signals are obtained according to the normal static force sensor and eddy current displacement sensor. These signals are transmitted to the test and analysis system through the amplifier, and finally realize the data acquisition of the static force and deformation of the joint surface.

(a)The experimental box   (b) The layout of sensors
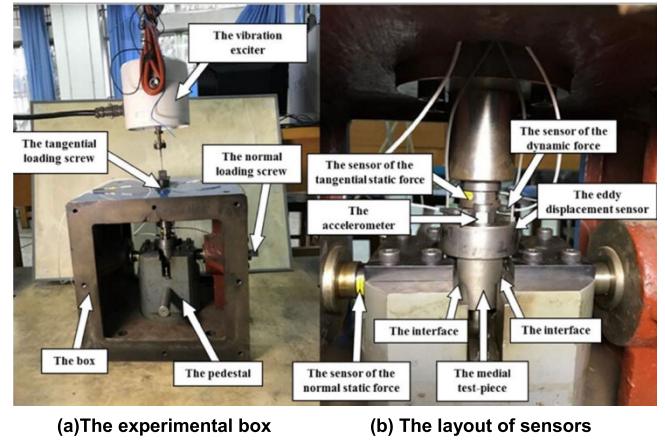
FIGURE 8. Experimental device of the tangential contact stiffness.

From the test system, we can read a series of normal static load values $P_{n1}, P_{n2}, \cdots \cdots P_{nn}$ and tangential static load values, as well as the tangential relative displacement average (average value of two eddy current displacement sensors) $\lambda_{\tau 1}, \lambda_{\tau 2}, \cdots \cdots \lambda_{\tau n}$ corresponding to $P_{\tau 1}, P_{\tau 2}, \cdots \cdots P_{\tau n}$.

Then the normal contact surface pressure of the bonding surface is:

$$p_n = \frac{4P_n}{\pi d^2} \qquad (29)$$

where is the diameter of the contact surface of the left and right specimen, its value is 30 mm; the tangential contact surface pressure of the bonding surface is:

$$p_\tau = \frac{4P_\tau /2}{\pi d^2} \qquad (30)$$

As a result, a set of experimental values $(p_{\tau 1}, \lambda_{\tau 1}), (p_{\tau 2}, \lambda_{\tau 2}), \cdots \cdots (p_{\tau n}, \lambda_{\tau n})$ can be obtained. The tangential stiffness can be calculated to be

$$k_\tau = \frac{\Delta p_\tau}{\Delta \lambda_\tau} \qquad (31)$$

According The experiment adopts the same system conditions as the simulation, the upper/lower specimen test material is 45 steel, milling, the material property parameter is $E_1 = E_2 = 2.07 \times 10^{11}$ Pa, Poisson's ratio $v_1 = v_2 = 0.29$, the yield strength of the material is $p_y = 18$ GPa. Using the method of taking the surface parameters of the test specimen in Reference [38], it is found that the statistical parameter of

the micro-morphology of the contact surface is dd, plasticity index ff. It is assumed that the height of the asperity is a Gaussian distribution. Kunlun engine oil is selected as the lubricating medium of solid-liquid interface. Its SAE viscosity is 5W-40 and its dynamic viscosity is 82.4 mm²/s at 40 °C. Under the above conditions, the tangential stiffness experiments of solid-liquid bonding surface with and without lubricating medium were carried out respectively.

Figure 9 (a-b) reveals the relationship between tangential plane pressure and tangential displacement of solid-solid interface and solid-liquid interface under different normal plane pressure, respectively. It can be seen from the figure that the relationship between the tangential plane pressure and the relative displacement of the joint plane is approximately straight line. The greater the normal surface pressure, the smaller the slope of the straight line, because the greater the normal surface pressure, the more asperity bodies in contact with the bonding surface, and the stronger the ability to resist deformation under the same tangential load, the smaller the relative displacement.
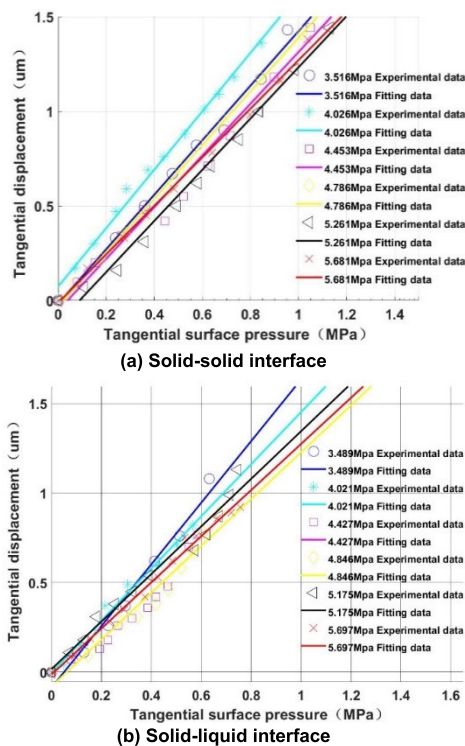
FIGURE 9. Relationship between tangential surface pressure and tangential displacement.

Figure 10 indicates the relationship between tangential static contact stiffness of solid-solid interface and solid-liquid interface with normal surface pressure, and the experimental data are fitted by power approximation. It can be seen from the diagram that the tangential static stiffness of the solid-solid and solid-liquid interface increases nonlinearly with the normal surface pressure, and the tangential static stiffness of the solid-liquid interface is larger than that of the

solid-liquid interface at low normal surface pressure. With the increase of normal surface pressure, the two gradually coincide. This is because when the normal surface pressure is low, the lubricant still exists in the contact interface, and because of its stiffness contribution, the solid-liquid interface is higher than the solid-solid interface, and with the increase of the normal surface pressure, the lubricant is extruded from the interface, the liquid contact area becomes smaller, and the contact area is almost completely occupied by asperity bodies, so the two are gradually equal.

Figure 11 shows the comparative analysis of the theoretical model curve and the experimental data point of the static tangential contact stiffness of solid-liquid interface and solid-solid interface with normal surface pressure. It can be seen from the figure that the changing trend of the experimental data points of the static contact model is the same as that of the theoretical model, and the static tangential contact stiffness increases nonlinearly with the normal surface pressure, indicating the correctness of the theoretical model.
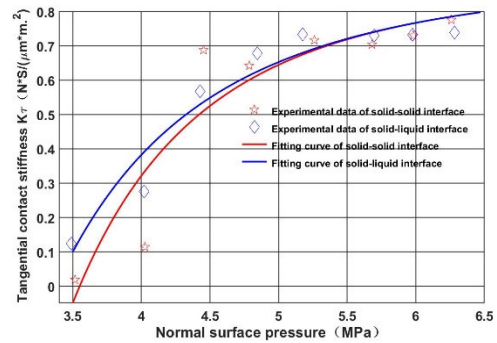
FIGURE 10. Variation of tangential stiffness with normal surface pressure.
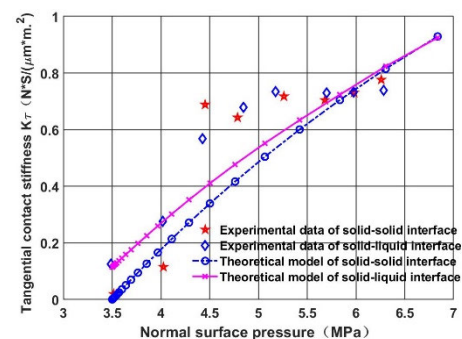
FIGURE 11. Theoretical and experimental comparison of the relationship between tangential contact stiffness and normal surface pressure.

VII. CONCLUSION
In the state of mixed lubrication, the tangential contact characteristics of the bonding surface are affected by the lubricating medium. In this article, a tangential contact stiffness model of mixed lubrication considering elastic-plastic deformation of asperities is established based on solid

elasto-plastic theory and liquid closed oil pit theory. The effects of normal load, normal deformation and lubricating oil viscosity on the tangential contact stiffness of mixed lubrication interface are analyzed, and the contact characteristics of solid-solid interface and solid-liquid interface are compared. The validity of the theoretical model is verified by experiments.

The main results are summarized as follows:

(1) The tangential contact characteristics of solid-liquid interface and solid-solid interface are similar, and both increase nonlinearly with the increase of normal load and deformation. Due to the contribution of liquid contact stiffness, the tangential stiffness of solid-liquid interface is always slightly higher than that of solid-solid interface.

(2) When the normal deformation is the same, the greater the viscosity of the lubricant, the greater the tangential contact stiffness of the solid-liquid interface.

(3) When the normal load or deformation is small, the tangential contact stiffness of the liquid closed oil pit is dominant, and the overall tangential stiffness of the solid-liquid interface is very small. With the gradual application of normal load, the contact characteristics of solid-liquid interface are mainly dominated by the solid contact part, and the tangential contact stiffness of solid-liquid interface increases rapidly. The normal load continues to increase, and the stiffness variation curve of solid-solid interface and solid-liquid interface gradually approaches to coincidence. Therefore, the static tangential contact stiffness of the solid-liquid interface under mixed lubrication is mainly determined by the solid-solid contact state, and the influence of lubricating film is limited.

REFERENCES

[1] Z. Q. Gao, Y. P. Xi, L. X. Peng, W. P. Fu, W. Wang, and S. Q. Wang, "Study on normal contact stiffness of non-Gaussian surface undermixed lubrication," *Mech. Sci. Technol. Aerosp. Eng.*, Jan. 2023, doi: 10.13433/j.cnki.1003-8728.20230035.

[2] H. Xiao, Y. Sun, J. Xu, and Y. Shao, "A calculation model for the normal contact stiffness of rough surface in mixed lubrication," *J. Vib. Shock*, vol. 37, no. 24, pp. 106–114, 2018.

[3] A. Carrelle, M. J. Bennan, T. P. Waters, and V. Lopes, "Force and displacement transmissibility of a nonlinear isolator with high-static-low-dynamic-stiffness," *Int. J. Mech. Sci.*, vol. 55, no. 1, pp. 22–29, Feb. 2012.

[4] H. T. Zou and B. L. Wang, "Investigation of the contact stiffness variation of linear rolling guides due to the effects of friction and wear during operation," *Tribol. Int.*, vol. 92, pp. 472–484, Dec. 2015.

[5] X. Li, "Influence of surface topography characteristics on mode coupling instability system," *J. Mech. Eng.*, vol. 53, no. 5, pp. 116–127, 2017.

[6] Z. Q. Gao, "Study on the theoretical model of contact stiffness and damping of mechanical joint," M.S. thesis, Xi'an Univ. Technol., Xi'an, China, Nov. 2018.

[7] H. G. Li, H. Liu, and L. Yu, "Contact stiffness of rough mechanical joint surface," *J. Xi'an Jiaotong Univ.*, vol. 45, no. 6, pp. 69–74, Jun. 2011.

[8] X. L. Zhang and S. H. Wen, "A fractal model of tangential contact stiffness of joint surfaces based on the contact fractal theory," *Trans. Agricult. Machinery*, vol. 33, no. 3, pp. 91–93, 2002.

[9] V. Brizmer, Y. Kligerman, and I. Etsion, "Elastic-plastic spherical contact under combined normal and tangential loading in full stick," *Tribol. Lett.*, vol. 25, no. 1, pp. 61–70, Dec. 2006.

[10] I. I. Argatov and E. A. Butcher, "On the Iwan models for lap-type bolted joints," *Int. J. Non-Linear Mech.*, vol. 46, no. 2, pp. 347–356, Mar. 2011.

[11] J. Shi, X. Cao, and H. Zhu, "Tangential contact stiffness of rough cylindrical faying surfaces based on the fractal theory," *J. Tribol.*, vol. 136, no. 4, pp. 919–927, Oct. 2014.

[12] Y. Sun, H. Xiao, J. Xu, and W. Yu, "Study on the normal contact stiffness of the fractal rough surface in mixed lubrication," *J. Eng. Tribol.*, vol. 232, no. 12, pp. 1604–1617, Dec. 2018.

[13] G. Cheng, K. Xiao, and J. Wang, "Contact damping and stiffness calculation model for rough surface considering lubrication in involute spur gear," *Int. J. Appl. Mech.*, vol. 13, no. 7, Aug. 2021, Art. no. 2150078.

[14] Z. Wang, W. Pu, X. Pei, and W. Cao, "Contact stiffness and damping of spiral bevel gears under transient mixed lubrication conditions," *Friction*, vol. 10, no. 4, pp. 545–559, Apr. 2022.

[15] R. S. Dwyer-Joyce, T. Reddyhoff, and J. Zhu, "Ultrasonic measurement for film thickness and solid contact in elastohydrodynamic lubrication," *J. Tribol.*, vol. 133, no. 3, pp. 407–411, Jul. 2011.

[16] H. Xiao, Y. Sun, and J. Xu, "Investigation into the normal contact stiffness of rough surface in line contact mixed elastohydrodynamic lubrication," *Tribol. Trans.*, vol. 61, no. 4, pp. 742–753, Jul. 2018.

[17] G. Cheng, K. Xiao, J. Wang, W. Pu, and Y. Han, "Calculation of gear meshing stiffness considering lubrication," *J. Tribol.*, vol. 142, no. 3, Mar. 2020, Art. no. 031602.

[18] C. Zhou, Z. Xiao, S. Chen, and X. Han, "Normal and tangential oil film stiffness of modified spur gear with non-newtonian elastohydrodynamic lubrication," *Tribol. Int.*, vol. 109, pp. 319–327, May 2017.

[19] C. Zhou and Z. Xiao, "Stiffness and damping models for the oil film in line contact elastohydrodynamic lubrication and applications in the gear drive," *Appl. Math. Model.*, vol. 61, pp. 634–649, Sep. 2018.

[20] R. E. Jones, "A greenwood-williamson model of small-scale friction," *J. Appl. Mech.*, vol. 74, no. 1, pp. 31–40, Jan. 2007.

[21] T. Sobis, U. Engel, and M. Geiger, "A theoretical study on wear simulation in metal forming processes," *J. Mater. Process. Technol.*, vol. 34, nos. 1–4, pp. 233–240, Sep. 1992.

[22] Y. Kadin, Y. Kligerman, and I. Etsion, "Unloading an elastic-plastic contact of rough surfaces," *J. Mech. Phys. Solids*, vol. 54, no. 12, pp. 2652–2674, Dec. 2006.

[23] L. Kogut and I. Etsion, "Elastic-plastic contact analysis of a sphere and a rigid flat," *J. Appl. Mech.*, vol. 69, no. 5, pp. 657–662, Sep. 2002.

[24] C. B. Ma, "Study on lubrication calculation model and antifriction characterists of textured surface," M.S. thesis, China Univ. Mining Technol., Beijing, China, Jun. 2010.

[25] W. P. Fu, L. T. Lou, Z. Q. Gao, W. Wang, and J. B. Wu, "Theoretical model of normal contact stiffness and damping of mechanical joint," *J. Mech. Eng.*, vol. 53, no. 9, pp. 73–82, 2017.

[26] T. Fujimoto, J. Kagami, T. Kawaguchi, and T. Hatazawa, "Microdisplacement characteristics under tangential force," *Wear*, vol. 241, no. 2, pp. 136–142, Jul. 2000.

[27] Y. Zhao and L. Chang, "A model of asperity interactions in elastic-plastic contact of rough surfaces," *J. Tribol.*, vol. 123, no. 4, pp. 857–864, Oct. 2001.

[28] C. Thornton and Z. Ning, "A theoretical model for the stick/bounce behaviour of adhesive, elastic-plastic spheres," *Powder Technol.*, vol. 99, no. 2, pp. 154–162, Sep. 1998.

[29] C. Thornton, Z. Ning, C. Y. Wang, M. Nasrullah, and L.-Y. Li, "Contact mechanics and coefficients of restitution," in *Granular Gases*. Berlin, Germany: Springer, 2001, pp. 184–194.

[30] C. Thornton, "Coefficient of restitution for collinear collisions of elastic-perfectly plastic spheres," *J. Appl. Mech.*, vol. 64, no. 2, pp. 383–386, Jun. 1997.

[31] S. M. He, S. Wu, and J. Shen, "Microscopic displacement characteristics of elastic-plastic materials under tangential load," *Eng. Mech.*, vol. 27, pp. 73–77, Feb. 2010.

[32] S. Z. Wen and P. Huang, *Principles of Tribology*, 2nd ed. Beijing, China: Qinghua Univ. Press, 2002.

[33] D. Dowson and G. R. Higginson, *Elasto-Hydrodynamic Lubrication*. London, U.K.: Pergamon Press, 1977.

[34] J. Hu and C. Wei, "Research on the friction behaviors of two rough surfaces covered with boundary film," *Tribol. Lett.*, vol. 53, no. 2, pp. 487–496, Feb. 2014.

[35] B. Zhao, F. Wu, K. Sun, X. Mu, Y. Zhang, and Q. Sun, "Study on tangential stiffness nonlinear softening of bolted joint in friction-sliding process," *Tribol. Int.*, vol. 156, Apr. 2021, Art. no. 106856.

[36] M. Rusli and M. Okuma, "Effect of surface topography on mode-coupling model of dry contact sliding systems," *J. Sound Vib.*, vol. 308, nos. 3–5, pp. 721–734, Dec. 2007.

[37] W. P. Fu, Z. Q. Gao, W. Wang, and J. B. Wu, "A model of tangential contact damping considering asperity interaction and lateral contact," *Acta Mechanica Solida Sinica*, vol. 31, no. 6, pp. 758–774, Dec. 2018.

[38] F. Van De Velde and P. De Baets, "The relation between friction force and relative speed during the slip-phase of a stick-slip cycle," *Wear*, vol. 219, no. 2, pp. 220–226, Sep. 1998.

LIXIA PENG received the M.S. degree from the Lanzhou University of Technology, Lanzhou, China, in 2009. She is currently pursuing the Ph.D. degree in mechanical engineering with the Xi'an University of Technology. She is also a Professor with Xi'an International University. Her primary research interests include intelligent robotics and mechanical system dynamics.

WEIPING FU received the Ph.D. degree from Xi'an Jiaotong University, Xi'an, China, in 1996. He is currently a Professor with the Xi'an University of Technology, Xi'an. He was the Standing Director of the Shaanxi Vibration Engineering Society and Xi'an Vibration and Noise Society. He mainly engaged in the research of intelligent robot, logistics automation, and intelligent manufacturing. He is a member of China Computer Society.

ZHAOYANG BAN received the M.S. degree from the Xi'an University of Technology, Shannxi, China, in 2021. He is currently a Engineer with Xi'an Lingkong Electronic Technology Company Ltd. His research is mainly on mechanical system dynamics.

FENG GAO received the Ph.D. degree from the Xi'an University of Technology, Xi'an, China, in 2001. He is currently a Professor with the Xi'an University of Technology. His research interests include CNC equipment design and control technology, virtual prototype simulation technology of CNC machine tools, on-machine testing technology of CNC machine tools, and error compensation theory.

ZHIQIANG GAO received the Ph.D. degree from the Xi'an University of Technology, Xi'an, China, in 2018. His research interests include mechanical optimization and dynamics analysis and the intelligent loading and unloading system of robot.

WEN WANG received the B.S. degree from Nanchang Hangkong University, Nanchang, China, in 1987, and the M.S. and Ph.D. degrees from the Xi'an University of Technology, Xi'an, China, in 2004 and 2010, respectively. She is currently a Professor with the Xi'an University of Technology. Her current research interests include intelligent robotics and modern logistics system engineering.

• • •